

**LOW-ORBITAL TRANSFORMABLE NANOSATELLITE:
RESEARCH OF THE DYNAMICS AND POSSIBILITIES
OF NAVIGATIONAL AND COMMUNICATION PROBLEMS
SOLVING FOR PASSIVE AERODYNAMIC STABILIZATION**

I.V. Belokonov,^{*} A.V. Kramlikh,[†] I.A. Timbai[‡]

In this paper the uncontrolled motion about the mass center of aerodynamically stabilized nanosatellite with transformable structure moving along the LEO circular orbit was considered. As a result of the construction transformation, static stability is increased. The analytical cumulative distribution function and the probability density function of the maximum nanosatellite angle of attack for Rayleigh and uniform distributions of the initial transverse angular velocity value for the nanosatellite planar motion are obtained. The distribution laws of the maximum of nanosatellite attack angle after transformation are obtained by numerical simulations for the case of spatial motion. Using found distribution laws of the maximum of nanosatellite attack angle it is analyzed the possibility of successful solutions of navigational problems connected with the use of satellite radio navigation systems GLONASS/GPS and low-altitude satellite communication network GlobalStar. The obtained results are used to create nanosatellite SamSat-QB50 as the part of the international project QB50.

INTRODUCTION

Small satellites often use passive or combined (passive in combination with active) orientation systems to ensure the desired own orientation. An important task in creating any passive attitude control system is to study the uncontrolled motion of the satellite concerning the mass center, so as to ensure the estimated motion conditions such satellites is carried out only at the design stage by choosing its design and ballistic parameters, as well as specifying limits on the angular velocity generated by the separation system. To study the possibility of successful solutions of navigation and communication problems on board is also an essential task in process of uncontrolled motion relative to the satellite mass center. A similar problem was considered in the article (Reference 1) for the upper stage of carrier rocket "Soyuz", engages in uncontrolled motion after payload separation which formed the stochastic models of the initial conditions of its angular motion and it was determined the probability of successful solutions of the navigation and communication problems. In paper (Reference 2) for low near-circular orbit it has been investigated uncontrolled motion relative to the mass center of nanosatellite standard CubeSat-2U rotating around the longitudinal axis, formed stochastic models of the initial conditions of nanosatellite angular motion, analyzed the possibility of solving the radionavigation tasks.

^{*} Professor, Dr. of Eng. Sci., Head of Space Research Department of the Samara State Aerospace University, Russia, E-mail: ibelokonov@mail.ru

[†] Candidate of Eng. Sci., Samara State Aerospace University, Russia, E-mail: kramlikh@mail.ru.

[‡] Professor, Dr. of Eng. Sci., Samara State Aerospace University, Russia, E-mail: timbai@mail.ru.

In this paper, the uncontrolled motion of aerodynamically stabilized nanosatellite with transformable structure moving along a low circular orbit. It is investigated the nature of the motion dynamics and evaluated the possibility of solving problems connected with navigation and communication on nanosatellite board when its passive stabilization is under the action of aerodynamic forces. As an example it is considered a 2 kg nanosatellite having CubeSat 2U original shape with dimensions of $20 \times 10 \times 10$ cm, the longitudinal moment of inertia $J_x = 0.0033 \text{ kg m}^2$, the transverse moment of inertia $J_y = J_z = J_n = 0.0083 \text{ kg m}^2$, the initial distance between the center of pressure and mass center is 1 cm. After separation from the adapter nanosatellite transforms into CubeSat 3U form with dimensions $30 \times 10 \times 10$ cm, thereby significantly increasing the distance between the center of pressure and mass center (up to 5.5 cm), also changes the transverse moment of inertia $J_n = 0.012 \text{ kg m}^2$. It should be noted that according to the law of kinematic momentum conservation, in case of the nanosatellite transformation the transverse angular velocity due to error separation system decreases in 1.4 times.

MOMENTS ACTING ON THE NANOSATELLITE

There are main moments acting on nanosatellite (gravitational and aerodynamic) in comparison in the article. If nanosatellite transformation increases the difference transverse and longitudinal inertia moments it leads to an increase of the gravitational moment acting on nanosatellite in 1.7 times. The change in the aerodynamic moment by transforming nanosatellite is determined. It was decided that the nanosatellite wrapping is free-molecule and the gas molecules collision is perfectly inelastic, the resultant aerodynamic forces is applied to the nanosatellite geometric center. In this case, the aerodynamic drag force is determined by the nanosatellite area projected on a plane, normalized with respect to the flow velocity vector³ and the restoring aerodynamic moment coefficient is determined by the formula:

$$m_\alpha(\alpha, \varphi) = -c_0 \tilde{S}(\alpha, \varphi) \Delta \bar{x} \sin(\alpha), \quad (1)$$

where $c_0 = 2.2$ is drag force coefficient; $\Delta \bar{x} = x_g / l$ is static stability factor, x_g is the mass center, measured from the nanosatellite geometric center, l is nanosatellite characteristic length (up to transformation $l=0.2$ m, after transformation $l=0.3$ m); $\tilde{S} = |\cos(\alpha)| + k |\sin(\alpha)| \cdot (|\sin(\varphi)| + |\cos(\varphi)|)$ is nanosatellite area projected on a plane, normalized with respect to flow velocity vector divided by the characteristic nanosatellite square $S=0.01 \text{ m}^2$, k is the ratio of the one of the side surfaces area in a characteristic space (before transformation $k=2$, after transformation $k=3$), α is spatial angle of attack (the angle between the longitudinal axis and nanosatellite mass center velocity vector), φ is proper rotation angle (the angle between the angle of attack plane and the lateral axis, perpendicular with respect to the side).

In the Figures 1 and 2 there are shown the dependence of the restoring aerodynamic moment coefficient relative to the nanosatellite mass center $m_\alpha = m_\alpha(\alpha, \varphi)$ before transformation (Figure 1) and after transformation (Figure 2) on the spatial angle of attack α and angle of proper rotation φ . Curves 1 and 2 are constructed according to dependence m_α obtained for the angle of proper rotation values $\varphi = 0$ and $\varphi = 45$ degrees, respectively. For the qualitative analysis of the motion relative to the mass center dependence m_α is averaged over the angle of proper rotation φ (curve 3), and then approximated by a sine function of the angle of attack $a_0 \sin(\alpha)$

(dashed line in Figures 1 and 2, before the nanosatellite transformation coefficient $a_0 = -0.28$, after transformation - $a_0 = -1.5$).

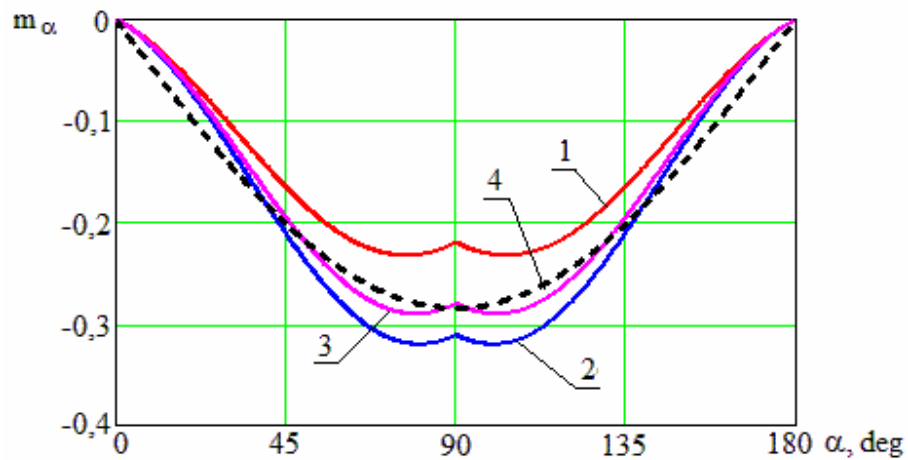


Figure 1. Dependence of restoring aerodynamic moment coefficient before transformation on spatial angle of attack and angle of proper rotation (1 - $\varphi = 0$, 2 - $\varphi = 45^\circ$, 3 - averaged over angle of proper rotation φ , 4 - approximated by sinusoidal dependence).

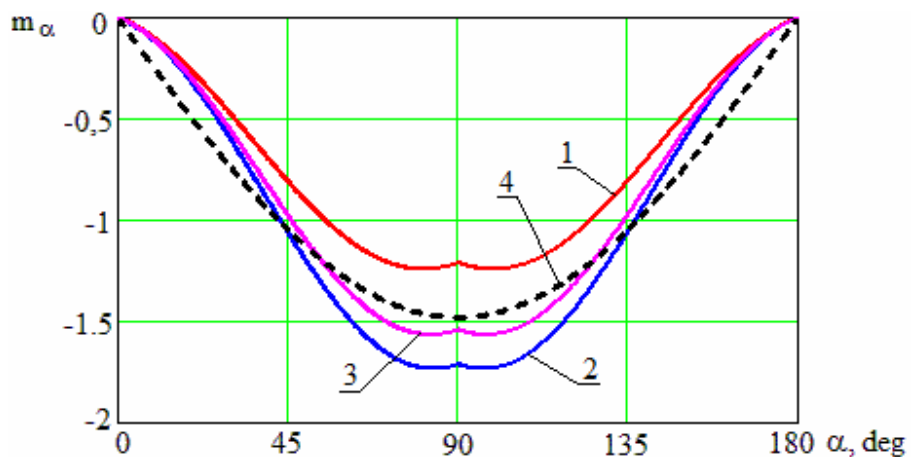


Figure 2. Dependence of restoring aerodynamic moment coefficient after transformation on spatial angle of attack and angle of proper rotation (1 - $\varphi = 0$, 2 - $\varphi = 45^\circ$, 3 - averaged over angle of proper rotation φ , 4 - approximated by sinusoidal dependence).

Thus, due to transforming nanosatellite shape its aerodynamic moment increases in 8 times and gravitational - only in 1.7, that significantly expands range of altitude which can provide nanosatellite aerodynamic stabilization.

NANOSATELLITE PLANAR ANGULAR MOTION

It was executed a qualitative analysis of the motion about the nanosatellite mass center using an approximate model of angular motion in the plane of the circular orbit with respect to the trajectory reference frame. The model describes the change in the angle of attack by the gravitational and restoring aerodynamic moment by equation³ :

$$\ddot{\alpha} - a(H) \sin \alpha - c(H) \sin 2\alpha = 0, \quad (2)$$

where $a(H) = a_0 S l q(H) / J_n$ is coefficient associated with aerodynamic restoring moment; $q(H) = V^2 \rho(H) / 2$ is velocity head; V is flight speed; H is orbit altitude, $\rho(H)$ is atmospheric density; $c(H) = 3(J_n - J_x)(\omega(H))^2 / (2J_n)$ is coefficient associated with the gravitational moment; $\omega(H) = \sqrt{\mu / (R_E + H)^3}$ is the angular orbital velocity of the nanosatellite; R_E is radius of the spherical Earth; μ is Earth's gravitational parameter.

Changing the altitude of the circular orbit because of atmospheric drag is very slow and when considering the nanosatellite angular motion on one or more turns it can be taken $H = const$. In this case, the system (2) has an integral of energy:

$$\dot{\alpha}^2 / 2 + a \cos \alpha + c \cos^2 \alpha = E_0, \quad (3)$$

where $E_0 = a \cos \alpha_0 + c \cos^2 \alpha_0 + \frac{\dot{\alpha}_0^2}{2}$ determined by the initial conditions.

Character of nanosatellite motion is defined by the values a , c and E_0 . For the case $a < 0$, $c > 0$ there are two types of phase portraits.

1. $c > 0.5 |a|$. With such a ratio there are four areas of nanosatellite motion: rotational region and three oscillatory regions. Figure 3 shows the phase portrait of the nanosatellite motion after transformation at a height $H=600$ km. Nanosatellite has four equilibrium positions according to the angle of attack: $\alpha_* = \pm \arccos(-0.5a/c) + 2n\pi$ ($n = 0 \pm 1, \pm 2, \dots$), $\alpha = 0 + 2n\pi$ ($n = 0 \pm 1, \pm 2, \dots$), $\alpha = \pi + 2n\pi$ ($n = 0 \pm 1, \pm 2, \dots$). Rotational motion of the nanosatellite corresponds to the condition: $E_0 > -a + c$ - phase trajectory 1, oscillating around the equilibrium position $\alpha = 0 + 2n\pi$ ($n = 0 \pm 1, \pm 2, \dots$) corresponds to the condition: $-a + c < E_0 < a + c$ - phase trajectory 2, oscillating around the equilibrium position α_* corresponds to the condition: $E_0 < a + c$ - phase trajectory 3. Region of possible motions are divided by separatrices (in Figure 3 these are the phase trajectories 4 and 5).

2. $|a| \geq 2c$. Phase portrait is similar to an oscillating system of the pendulum type. Figure 4 shows the phase portrait of nanosatellite motion after transformation at a height $H= 330$ km. In this case, nanosatellite has two equilibria angle of attack: it is stable when $\alpha = 0 + 2n\pi$ ($n = 0 \pm 1, \pm 2, \dots$) and unstable when $\alpha = \pi + 2n\pi$ ($n = 0 \pm 1, \pm 2, \dots$). Rotational motion of the nanosatellite corresponds to condition: $E_0 > -a + c$ (phase trajectory 1), oscillatory motion of relatively stable equilibrium $\alpha = 0 + 2n\pi$ ($n = 0 \pm 1, \pm 2, \dots$) corresponds to the condition: $E_0 < -a + c$ (phase trajectory 2). Region of possible motions are divided by separatrix - phase trajectory 3.

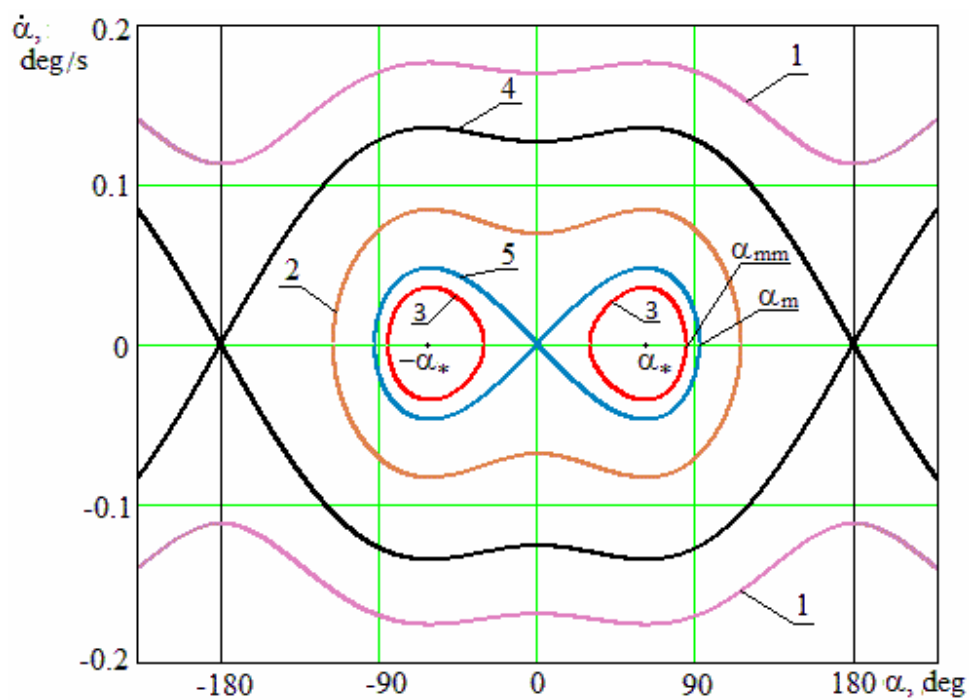


Figure 3. Phase portrait of the transformed nanosatellite motion at the flight altitude $H=600$ km.

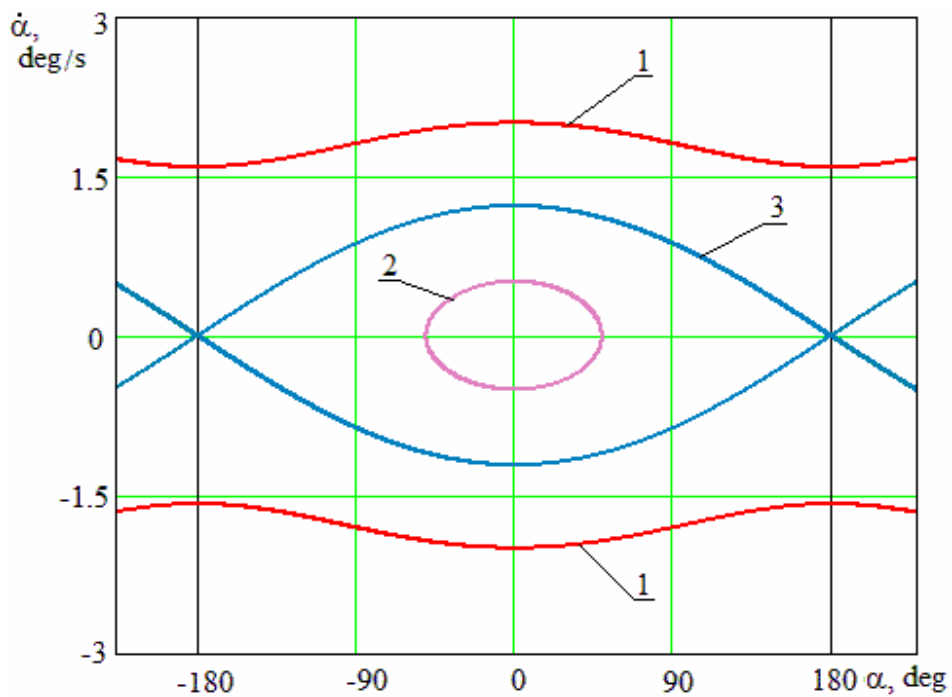


Figure 4. Phase portrait of the transformed nanosatellite motion at the flight altitude $H=330$ km.

With the increasing atmosphere density at lower altitude factor corresponded to aerodynamic restoring moment a is increased considerably, while the factor corresponded to the gravitational moment c virtually unchanged. If the motion began in the phase portrait shown in Figure 3, then when the condition is $|a| = 2c$ there is a change of the form of the phase portrait to the portrait depicted in Figure 4. Altitude of change of the phase portrait for the untransformed nanosatellite is $H=452$ km, for transformed is $H=554$ km at standard atmospheric density in accordance with standard GOST 4401-81 (Reference 4).

Also with nanosatellite altitude decreasing it is being changed the character of the phase trajectories, resulting in they can cross the separatrices, getting into various regions of the phase portrait that accompanied by qualitative changes in the nature of the motion: rotational motion becomes oscillatory, oscillatory motion abruptly goes to oscillate with other amplitude characteristics. For example, if initially the nanosatellite performs rotational motion, altitude H_* , corresponding to the transition of rotational motion into an oscillating, is determined from the solution of the transcendental equation⁵:

$$I_0 = 4\sqrt{2(c(H_*))}[\sqrt{u_* + 1} + u_* \ln((1 + \sqrt{u_* + 1})/\sqrt{u_*})],$$

where $u_* = |0.5a(H_*)/(c(H_*))|$; $I_0 = \int_{\alpha_{\min}}^{\alpha_{\max}} \dot{\alpha} d\alpha$ is action integral calculated from the initial conditions of motion; $\dot{\alpha}$ is determined from the integral of energy (3); α_{\min} , α_{\max} are amplitude values of the angle of attack (defined by (3) $\dot{\alpha} = 0$, during rotation $\alpha_{\min} = -\pi$, $\alpha_{\max} = \pi$).

If at the initial moment nanosatellite oscillates relative to the position of equilibrium α_* (Figure 3), the altitude H_* , corresponding to the time of transition to oscillations about the equilibrium position $\alpha = 0$, is determined from the solution of the transcendental equation⁵:

$$I_0 = 4\sqrt{2(c(H_*))}[\sqrt{1 - u_*} - u_* \ln((1 + \sqrt{1 - u_*})/\sqrt{u_*})].$$

Figure 5 shows the dependence of the transition altitude H_* of a rotational motion of the transformed nanosatellite into oscillations on values of initial angular velocity $\dot{\alpha}_0$ for different values of the initial angle of attack α_0 (initial altitude $H_0 = 330$ km).

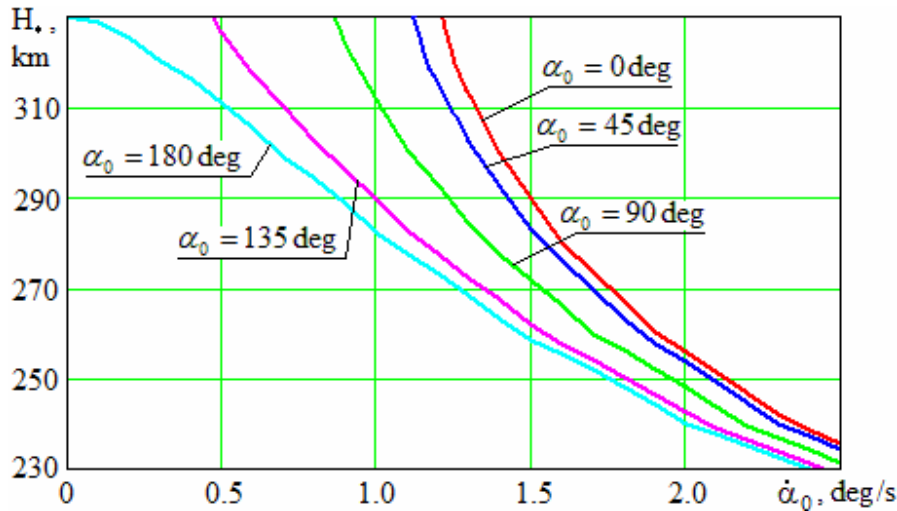


Figure 5. Altitude corresponding to the transition of rotational motion of transformed nanosatellite into oscillation one.

The value of the maximum angle of attack after separation of nanosatellite is random and determined by the initial value of the angle of attack α_0 , the initial value of the angular velocity $\dot{\alpha}_0$, aerodynamic and gravitational moments. Value of the maximum nanosatellite angle of attack with oscillations can be found from the integral of energy (3) provided that $\dot{\alpha} = 0$:

$$\cos \alpha_{\max} = -\frac{a}{2c} - \sqrt{\left(\frac{-a}{2c}\right)^2 + \frac{a}{c} \cos \alpha_0 + \cos^2 \alpha_0 + \frac{\dot{\alpha}_0^2}{2c}}. \quad (4)$$

Accepted, that among the quantities included in formula (4), the angular velocity $\dot{\alpha}_0$ has the largest range of values. Then, neglecting scatter of the other quantities it is appeared the laws of distribution of the maximum angle of attack for two variants of the magnitude distribution module $\dot{\alpha}_0$ - by Rayleigh law and uniform law.

Let the value $\dot{\alpha}_0$ distributed according to the Rayleigh law

$$f(\dot{\alpha}_0) = \frac{\dot{\alpha}_0}{\sigma^2} \exp\left(-\frac{\dot{\alpha}_0^2}{2\sigma^2}\right), \quad (5)$$

where $\sigma > 0$ is scale parameter of the distribution.

Then, calculating the distribution of function α_{\max} (4) over the argument distribution $\dot{\alpha}_0$ (5) in accordance with⁶, the analytical expressions for the probability density function and the cumulative distribution function of the maximum angle of attack are:

$$f(\alpha_{\max}) = \frac{-a \sin \alpha_{\max} - c \sin 2\alpha_{\max}}{\sigma^2} \exp\left(\frac{-a(\cos \alpha_{\max} - \cos \alpha_0) - c(\cos^2 \alpha_{\max} - \cos^2 \alpha_0)}{\sigma^2}\right), \quad (6)$$

$$F(\alpha_{\max}) = 1 - \exp\left(\frac{-a(\cos \alpha_{\max} - \cos \alpha_0) - c(\cos^2 \alpha_{\max} - \cos^2 \alpha_0)}{\sigma^2}\right). \quad (7)$$

Let the value $\dot{\alpha}_0$ distributed according to a uniform law in the range $[0, \dot{\alpha}_{0\max}]$:

$$f(\dot{\alpha}_0) = \begin{cases} \frac{1}{\dot{\alpha}_{0\max}}, & \dot{\alpha}_0 \in [0, \dot{\alpha}_{0\max}] \\ 0, & \dot{\alpha}_0 \notin [0, \dot{\alpha}_{0\max}] \end{cases}. \quad (8)$$

Then, calculating the distribution of function α_{\max} (4) over the argument distribution $\dot{\alpha}_0$ (5) in accordance with⁶, the analytical expressions for the probability density function and the cumulative distribution function of the maximum angle of attack are:

$$f(\alpha_{\max}) = \frac{-a \sin \alpha_{\max} - c \sin 2\alpha_{\max}}{\dot{\alpha}_{0\max} \sqrt{2a(\cos \alpha_{\max} - \cos \alpha_0) + 2c(\cos^2 \alpha_{\max} - \cos^2 \alpha_0)}}, \quad (9)$$

$$F(\alpha_{\max}) = \frac{\sqrt{2a(\cos \alpha_{\max} - \cos \alpha_0) + 2c(\cos^2 \alpha_{\max} - \cos^2 \alpha_0)}}{\dot{\alpha}_{0\max}}. \quad (10)$$

If the motion is in accordance with the phase portrait shown in Figure 3 (condition is $c > 0.5|a|$), the maximum angle of attack during oscillations can take the values of the ranges: (α_{mm}, π) if $\alpha_0 < \alpha_*$ and (α_0, π) if $\alpha_0 > \alpha_*$, where $\alpha_{mm} = \arccos(-a/c - \cos(\alpha_0))$ is minimum possible value of the maximum angle of attack with respect to oscillations in the equilibrium position α_* (see Figure 3). The probability of oscillations relative to the position of equilibrium α_* is calculated by formula

$$P_* = \begin{cases} F(\alpha_m), & \alpha_0 < \alpha_m \\ 0, & \alpha_0 > \alpha_m \end{cases}, \quad \text{where}$$

$\alpha_m = \arccos(-a/c - 1)$ is maximum possible value of the maximum angle of attack with respect to oscillations in the equilibrium position α_* (see Figure 3). Probability of oscillations relative to equilibria $\alpha = 0$ is equal to $P_0 = F(\pi) - F(\alpha_m)$. The probability of rotation is equal to $P_r = 1 - F(\pi)$.

If the motion is in accordance with the phase portrait shown in Figure 4 (condition is $|a| \geq 2c$), the maximum angle of attack during oscillations can take values from the range (α_0, π) . In this case, the probability of oscillations relative to equilibria $\alpha = 0$ is equal to $P_0 = F(\pi)$, and the probability of the rotation is $P_r = 1 - F(\pi)$.

NANOSATELLITE SPATIAL MOTION

There is the analysis of spatial motion about the mass center of the transformed nanosatellite on the altitudes, where the aerodynamic moment is predominant. For example, at an altitude of 330 km (altitude, which in 2015 is scheduled to orbit 50 nanosatellite standard CubeSat in the frame of the European project QB50) ratio of maximum aerodynamic moment to the maximum value of the gravitational moment equals to 41. Then, neglecting the influence of the gravitational moment and the orbital angular velocity, change of the spatial angle of attack of nanosatellite can be described by the following equation⁷:

$$\ddot{\alpha} + (G - R \cos \alpha)(R - G \cos \alpha) / \sin^3 \alpha - a(H) \sin \alpha = 0, \quad (11)$$

where $R = J_x \omega_x / J_n = \text{const}$, $G = R \cos \alpha + (-\omega_y \cos \varphi + \omega_z \sin \varphi) \sin \alpha = \text{const}$ are projections of the kinetic moment vector on the nanosatellite longitudinal axis and the direction of the velocity of the mass center, normalized with respect to the transversal moment of inertia, respectively; $\omega_x, \omega_y, \omega_z$ are components of the angular velocity in the body-fixed frame of reference.

Precession of the longitudinal axis of the nanosatellite about the mass center velocity in the time interval equal to the period of a complete revolution and the opposite direction to a given vector is called “inverse” precession, and coinciding with the direction of the velocity vector of the center of mass is called a “direct” precession⁸. Under the condition $R > G$ is implemented the “inverse” precession, when the condition $G > R$ is implemented the “direct” precession (see Figure 6).

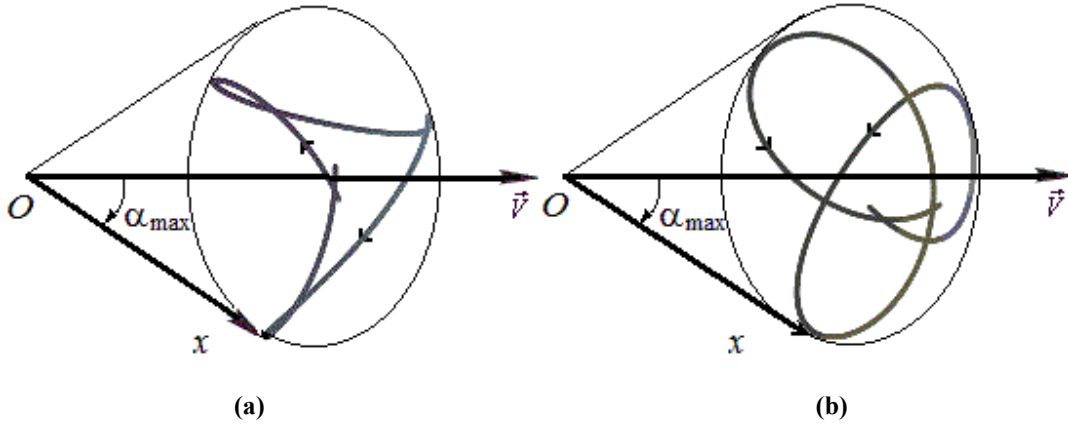


Figure 6. Trajectory of the end of the nanosatellite longitudinal axis on the unit sphere concerning the trajectory reference frame: (a) "inverse" precession, (b) "direct" precession.

When considering the nanosatellite angular motion it can be taken $H = const$. In this case for the system (11) is performed the integral of energy:

$$\dot{\alpha}^2 / 2 + (R^2 + G^2 - 2RG \cos \alpha) / (2 \sin^2 \alpha) + a \cos \alpha = E. \quad (12)$$

The value E is determined by the initial conditions, where $\dot{\alpha}_0 = \omega_y \cos \varphi_0 + \omega_z \sin \varphi_0$.

Maximum angle of attack is determined from the equation

$$(R^2 + G^2 - 2RG \cos \alpha_{\max}) / (2 \sin^2 \alpha_{\max}) + a \cos \alpha_{\max} - E = 0, \quad (13)$$

which follows from the integral of energy (12) for $\dot{\alpha} = 0$.

To determine the distribution function of the maximum nanosatellite angle of attack in the case of spatial motion it was conducted statistical modeling (10000 numerical experiments) by formula (13). It was assumed that the initial value of the angle of its own rotation is distributed uniformly in the range $[0, \pi]$ and at the initial time the longitudinal axis of nanosatellite is directed along the vector velocity of the mass center ($\alpha_0 \approx 0$), initial altitude is $H_0 = 330$ km. There are two variants of the distribution of vector components of the initial angular velocity of nanosatellite. For the first variant the initial angular velocity components of nanosatellite are independent and normally distributed with zero expectations (the value of the angular transversal velocity has Rayleigh distribution). For the second variant the value of transverse angular velocity and value longitudinal angular velocity are independent and uniformly distributed.

Figure 7 shows the change in the cumulative distribution function of the maximum angle of attack of nanosatellite depending on the values of mean square deviations σ of the initial of the angular velocity components after its transformation (initial angular velocity components are normally distributed): curve 1 corresponds to $3\sigma_{\omega_y} = 3\sigma_{\omega_z} = 0.5$ deg/s, $3\sigma_{\omega_x} = 0.1$ deg/s; curve 2 - $3\sigma_{\omega_y} = 3\sigma_{\omega_z} = 1.0$ deg/s, $3\sigma_{\omega_x} = 0.2$ deg/s; curve 3 - $3\sigma_{\omega_y} = 3\sigma_{\omega_z} = 1.5$ deg/s, $3\sigma_{\omega_x} = 0.3$ deg/s; curve 4 - $3\sigma_{\omega_y} = 3\sigma_{\omega_z} = 2.0$ deg/s, $3\sigma_{\omega_x} = 0.4$ deg/s; curve 5 - $3\sigma_{\omega_y} = 3\sigma_{\omega_z} = 2.5$ deg/s, $3\sigma_{\omega_x} = 0.5$ deg/s.

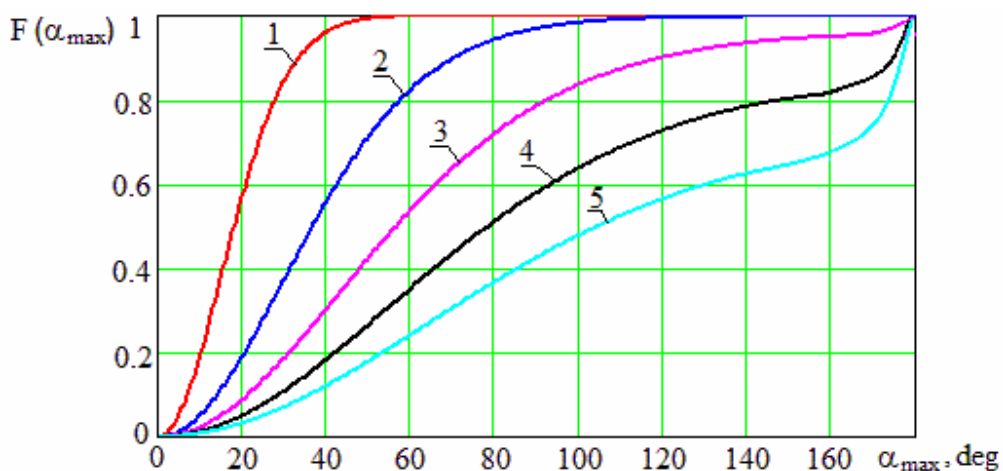


Figure 7. Cumulative distribution function of the maximum angle of attack of the nanosatellite (initial angular velocity components are normally distributed).

Figure 7 shows the variation of the cumulative distribution function of the maximum angle of attack of nanosatellite depending on the range of possible values of the components of the initial angular velocity (transverse and longitudinal angular velocities are distributed in a uniform law): curve 1 for $\omega_n \in [0; 0.5]$ deg/s, $\omega_x \in [0; 0.1]$ deg/s; curve 2 for $\omega_n \in [0; 1.0]$ deg/s, $\omega_x \in [0; 0.2]$ deg/s; curve 3 for $\omega_n \in [0; 1.5]$ deg/s, $\omega_x \in [0; 0.3]$ deg/s; curve 4 for $\omega_n \in [0; 2.0]$ deg/s, $\omega_x \in [0; 0.4]$ deg/s; curve 5 for $\omega_n \in [0; 2.5]$ deg/s, $\omega_x \in [0; 0.5]$ deg/s.

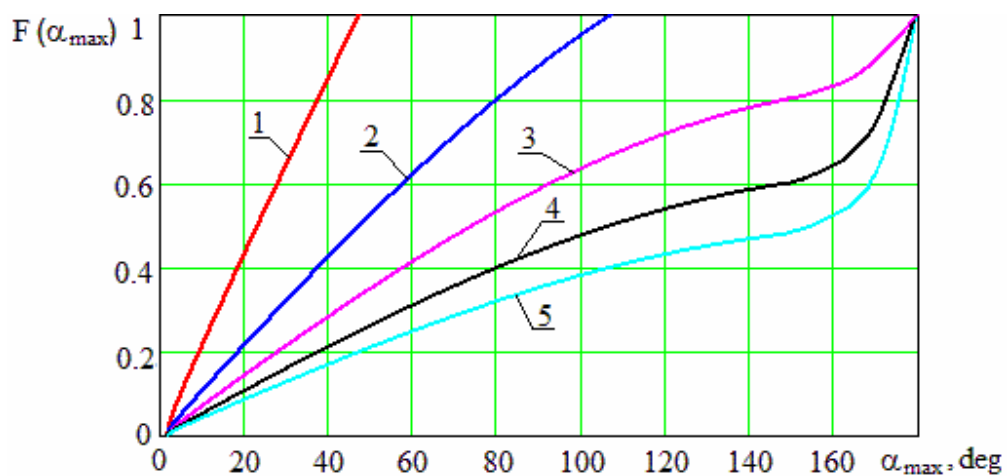


Figure 8. Cumulative distribution function of the maximum angle of attack of the nanosatellite (longitudinal and transverse angular velocities are distributed in a uniform law).

For small R and G (with a small difference between R and G , small initial value of angle of attack α_0) the formula (13) can be written as

$$a \cos \alpha_{\max} - E = 0, \quad (14)$$

where $E = a \cos \alpha_0 + \frac{\dot{\alpha}_0^2}{2}$.

From formula (14) it follows that $\cos \alpha_{\max} = \cos \alpha_0 + \frac{\dot{\alpha}_0^2}{2a}$. This corresponds to the planar case of motion under the influence of aerodynamic moment.

There is the estimation error using analytical cumulative distribution functions of the maximum angle of attack (obtained for a plane angular motion - the formula (6) and (8) with $c = 0$) depending on initial angle of attack α_0 and the initial longitudinal angular velocity ω_x in case of spatial motion.

Graph of analytical cumulative distribution function (7) (curve 1) and graphs of cumulative distribution function of the maximum angle of attack α_{\max} , obtained by numerical experiments on the formula (13) (curve 2 for $3\sigma_{\omega_x} = 0.5$ deg/s, curve 3 for $3\sigma_{\omega_x} = 1.5$ deg/s, curve 4 for $3\sigma_{\omega_x} = 2.5$ deg/s) are shown on Figures 9 and 10 for the case when the components of the initial transverse angular velocity are normally distributed $3\sigma_{\omega_y} = 3\sigma_{\omega_z} = 2.5$ deg/s, and the initial angle of attack is $\alpha_0 = 1$ degree (Figure 9) and $\alpha_0 = 15$ degrees (Figure 10).

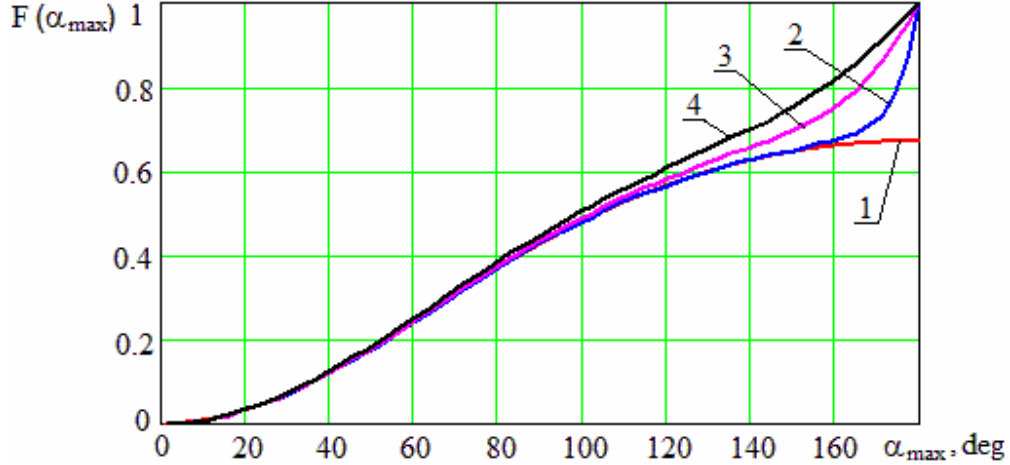


Figure 9. Cumulative distribution function of the maximum angle of attack ($\alpha_0 = 1$ deg).

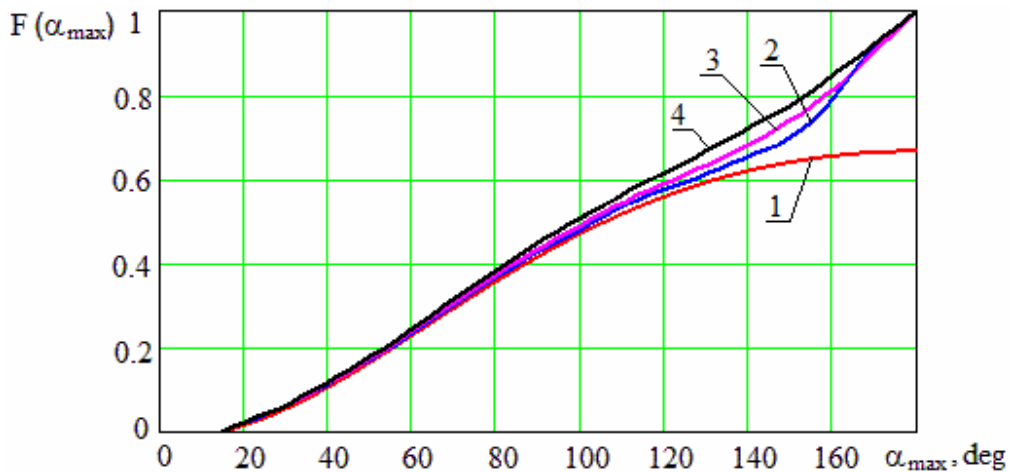


Figure 10. Cumulative distribution function of the maximum angle of attack ($\alpha_0 = 15$ deg).

As follows from the obtained results for the separation of nanosatellite along the vector velocity (the initial value of the angle of attack is small) and small spinning about the longitudinal axis can be used with sufficient precision analytical cumulative distribution function of the maximum angle of attack, obtaining in the case of plane angular motion, and case of spatial angular one. A similar conclusion can be drawn for the case where the longitudinal and transverse angular velocities are distributed in a uniform law.

RESEARCH OF THE SOLVING POSSIBILITY OF NANOSATELLITE NAVIGATION AND COMMUNICATION PROBLEMS

Success in solving of navigation and communication problems depends on the mode of uncontrolled motion and in particular on the maximum angle of attack (see Figure 6) which affects the size of the area of geometric visibility (cone angle of visibility) navigation and communication satellites from the nanosatellite. Therefore, obtained earlier distribution of the maximum angle of attack laws were used for the study of the possibility of successful solutions of the navigation-communication problems connected with the utilization of satellite navigation systems GLONASS/GPS and low-altitude satellite communication network GlobalStar.

Navigation solution is possible if there is continuous geometric visibility to the same satellites navigation constellation, the number of not less than three. The time interval of continuous visibility of the same satellites navigation constellation shall be not less than 90 s. The "full" navigation problem solution is understood as possibility of determination of three geocentric coordinates, three speed vector projections and time at continuous visibility not less than four navigation satellites. The "limited" navigation problem solution is understood as possibility of determination of three geocentric coordinates, three speed vector projections at continuous visibility not less than three navigation satellites.

Successful solution of communication problem is connected with geometric visibility of the same communication satellite in the required time interval (time interval is considered equal to 5 and 10 min, which are identical operating conditions with the ground mission control station).

Studying of the possibility of solving the nanosatellite navigation and communication problems was conducted with the following initial data:

- nanosatellite orbit is near-circular with an average altitude of 330 km, inclination is $i = 51^\circ$;
- nanosatellite separation is carried out on the vector of the center of mass velocity with minor spinning about the longitudinal axis (possible values do not exceed 2.5 deg/s);
- phase centers vectors of navigation and communication antennas are oriented along the nanosatellite longitudinal axis;
- beamwidth of antennas are equal 180° ;
- visibility cone angle of constellations of navigation and communication satellites on the side of the antenna phase center δ_c depends on the maximum angle of attack α_{\max} (Figure 6) and is determined by $\delta_c = 180^\circ - 2\alpha_{\max}$. For statistical modeling the angle implementation values α_{\max} are taken in accordance with the cumulative distribution functions (7), (10);
- the time interval is equal to period of nanosatellite motion on the circle orbit.

For studying of the solving of the navigation and communication problems is used statistical modeling and are considered two cases of the value distribution of the initial transverse angular velocity: Rayleigh distribution and uniform distribution.

To compute the probability solutions navigation and communication tasks it is used the total probability formula⁶

$$P(A_s) = \sum_{i=1}^n P(A_s | \delta_c^i) P(\delta_c^i), \quad (14)$$

where $P(A_s | \delta_c^i)$ is the conditional probability of navigation problem solution ($s = 1$) or a communication problem solution ($s = 2$), if there is the angle implementation δ_c^i ; $P(\delta_c^i)$ is the probability of visibility cone angle implementation δ_c^i .

In the Figure 11 there are the probabilities of navigation and communication problems solution depending on the tripled standard deviation value of the initial transverse angular velocity component (on the premise that magnitude of the initial transverse angular velocity has a Rayleigh distribution).

In the Figure 12 there are the probabilities of navigation and communication problems solution depending on the range of initial transverse angular velocity possible values (on the premise that value of the initial transverse angular velocity has a uniform distribution).

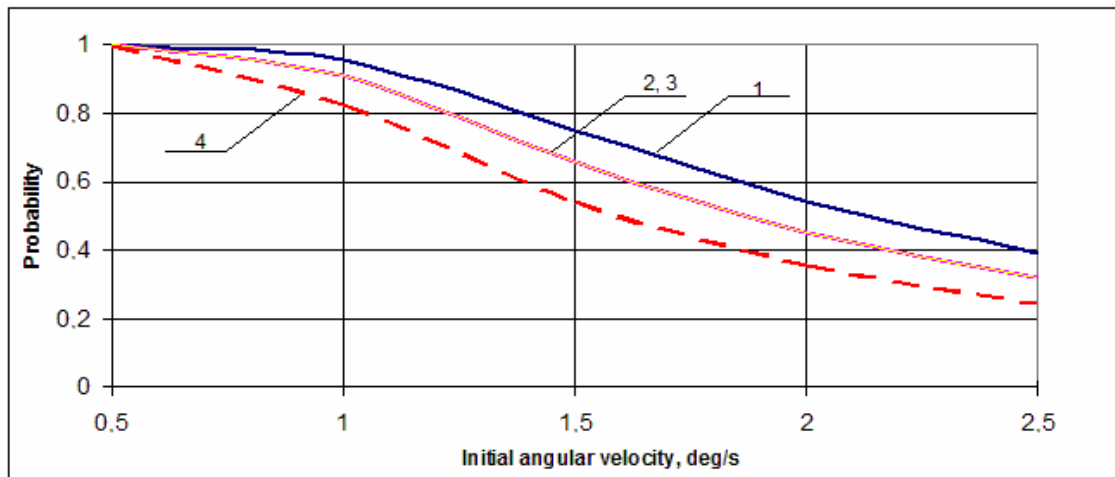


Figure 11. The probability of navigation and communication problems solution depending on the tripled standard deviation value of the initial transverse angular velocity component (1 – the "full" navigation task, 2 – the "limited" navigation task, 3 and 4 - communication tasks for the duration of the session 5 min and 10 min, respectively).

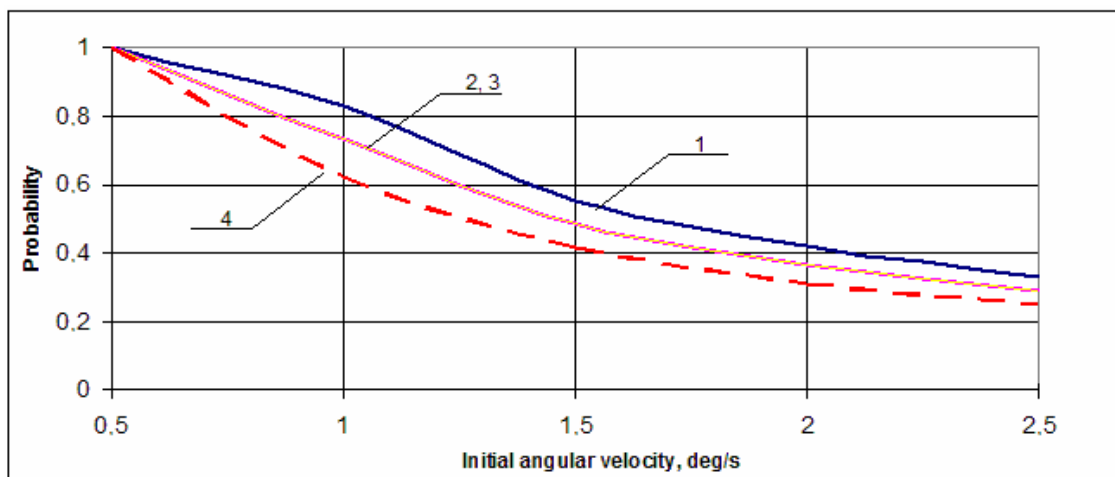


Figure 12. The probability of navigation and communication problems solution depending on the range of initial transverse angular velocity possible values (1 – the "full" navigation task, 2 – the "limited" navigation task, 3 and 4 - communication tasks for the duration of the session 5 min and 10 min, respectively).

As follows from the results, navigation and communication problems on board of transformed nanosatellite ($H = 300$ km) can be solved with the initial values of the transverse angular velocity of less than 0.5 deg/s. For large values of the initial angular velocity navigation and communication problems can be solved with a certain probability, for example, with a probability of 0.9 at angular velocities up to 0.8 deg/s. The admissible initial values of the angular velocities to be in-

creased by 1.4 times for the case of the separation of nanosatellite original form (CubeSat 2U). If the requirements for separation system to perform difficult, it is necessary to set damping devices, such as hysteresis rods, as the simplest and most reliable way to solve this problem^{9, 10}.

CONCLUSIONS

Thus, investigated the uncontrolled motion about the mass center of aerodynamically stabilized nanosatellite with transformable structure moving along the LEO circular orbit. The analytical cumulative distribution function and the probability density function of the maximum nanosatellite angle of attack for Rayleigh and uniform distributions of the initial transverse angular velocity value for the planar motion are obtained. The distribution laws of the maximum of nanosatellite attack angle after transformation are obtained by numerical simulations for the case of spatial motion. The possibility of solutions of navigational and communication problems connected with the use of satellite radio navigation systems GLONASS/GPS and low-altitude satellite communication network like GlobalStar are shown. The obtained results allow generating the limitations for errors in the angular velocity caused by utilized separation system of nanosatellites.

The results reflect general patterns of movement and the conditions for the realization of the mission aerodynamically stabilized transformable nanosatellite. The obtained results are used to create nanosatellite SamSat-QB50 (Reference 10) as the part of the international project QB50.

ACKNOWLEDGEMENT

The study was partially supported by RFBR, research project No. 13-08-97015- r_Volga region_a.

REFERENCES

- ¹ I.V. Belokonov, A.V Kramlikh, A.D Storozh and I.A. Timbay, Additional opportunities for carrying out of short term experiments on Soyuz orbital stages: communication and navigation problems, 63rd International Astronautical Congress, Naples, Italy, IAC-12-B2.5.9.
- ² I.V. Belokonov, A.V Kramlikh and I.A. Timbai, Radionavigation of low orbital CubeSat after separation from Soyuz upper stage: attitude motion influence, 7th International Workshop on Satellite Constellation and formation Flying, Lisbon, Portugal, 13-15 march 2013, IWSCFF-2013-08-04.
- ³ V.V. Beletsky, Motion of an satellite about its center of mass [in Russian], Nauka, Moscow, 1965.
- ⁴ GOST 4401-81 Standard atmosphere. Parameters, Moscow, 1981.
- ⁵ V.S. Aslanov and I.A. Timbay, Transient modes of spacecraft angular motion on the upper section of reentry trajectory, Cosmic Research, Vol.35, No. 3, 1997, pp. 260-267.
- ⁶ E.C. Wentzel and L.A. Ovcharov, Probability theory [in Russian], Fizmatgiz, Moscow, 1969.
- ⁷ V.A. Yaroshevsky, Motion of an uncontrolled body in the atmosphere [in Russian], Mashinostroenie, Moscow, 1978.
- ⁸ D.H. Platus, Angle of attack convergence windward meridian rotation rate of rolling re-entry vehicles, AIAA Journal, 1969, Vol.7, pp. 2324-2330
- ⁹ M.Yu.Ovchinnikov and V.I.Penkov, Passive Magnetic Attitude Control System for the Munin Nanosatellite, Cosmic Research, Vol.40, No. 2, 2002, pp. 142-156.
- ¹⁰ I. Belokonov, L. Gluhova, D. Ivanov, A. Kramlikh, M. Ovchinnikov, I. Timbai and E. Ustugov, Selection of Design Parameters of Aerodynamically Stabilized Nanosatellite for Thermosphere Research within the QB50 Project, 5th European CubeSat Symposium, 3 – 5 June 2013, Ecole Royale Militaire, Brussels, Book of Abstracts, p. 50.